DESIGN AND CONTROL OF A VIBRATING GYROSCOPE

Qais Khasawneh, C. Batur*

Department of Mechanical Engineering

University of Akron

Akron – Ohio

44325-3903

batur@uakron.edu

ABSTRACT

This paper presents design and control of a vibrating gyroscope. The MEMS based device has been designed in the Pro-E environment and simulated in a finite element domain in order to approximate its dynamic characteristics with a lumped model. The device is a modified version of the existing MEMS gyroscope proposed in [2]. An adaptive control, which has similar characteristics as the one proposed in [3], is added in order to guarantee the stability of the gyroscope.

1. INTRODUCTION

The common challenge in most vibrating gyroscopes is the minimization of the coupling between the driving and sensing axes. Several different designs are proposed recently to improve the performance of the vibrating rate gyroscopes by minimizing this coupling. The second challenge, which concerns the controller design, is the fact that the quantity that one wants to measure, i.e. the angular velocity, is an unknown term when the controller is designed. There may also exist other disturbances affecting the Couette and squeeze film based damping which may change due to variations in temperature or operating conditions.

This paper studies the first two problems by improving the design of one of the MEMS gyroscope proposed in [2] by adding an adaptive controller similar to the one proposed in [3]. The controller guarantees the Lyapunov stability i.e., all signals in the system remain bounded. This study shows that the boundedness of signals does not guarantee a consistent estimate of the unknown angular velocity. A new technique is proposed to consistently estimate the unknown angular velocity of the MEMS gyroscope. Figure 1 shows the basic structure of the vibrating MEMS gyroscope as described by Yoichi et. al. in [2].

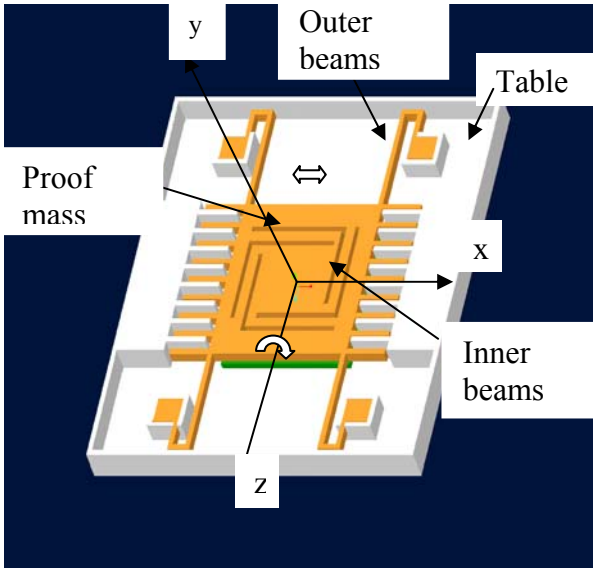

Fig.1: Assembly of the gyroscope, modified from reference [2].

The proof mass vibrates in x-direction and the angular velocity around z-direction is sensed by measuring the displacement of the proof mass in y-direction. In order to further reduce the coupling between the *x* and *y*-axes, slight modifications have been made on the dimensions of the outer beams and the thickness of the proof mass. The technical drawing of the modified design of [2] is shown in Figure 2. The proof mass has rectangular cross-sectioned comb fingers, which are aligned with another set of comb fingers anchored to the stationary part of the device.

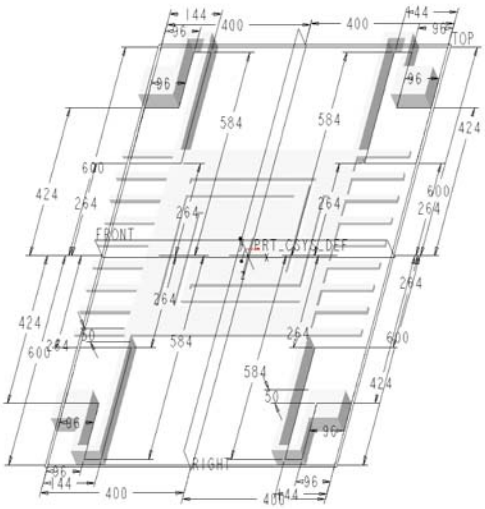

Fig. 2: Technical drawing of the gyroscope. All dimensions are in microns.

Four outer beams suspend the proof mass. In the original design [2], four inner beams are created by essentially cutting four legs on the proof-mass. The electro static force generated by the comb actuator vibrates the proof mass in *x*-direction. If the proof mass rotates with respect to z-axis, a Coriolis force is generated in the direction of the *y*-axis. This force moves the proof mass in the direction of the *y*-axis. The displacement in y-direction is proportional to the angular rate of rotation with respect to z-axis. The displacement is measured by the capacitance change in *y*-direction. Simulated motions of the device in *x* and *y* directions are shown in Figures 3 and 4, respectively [1]. All simulations are performed in Pro-E and Pro-Mechanica and they based on the technical drawing given in Figure 2.

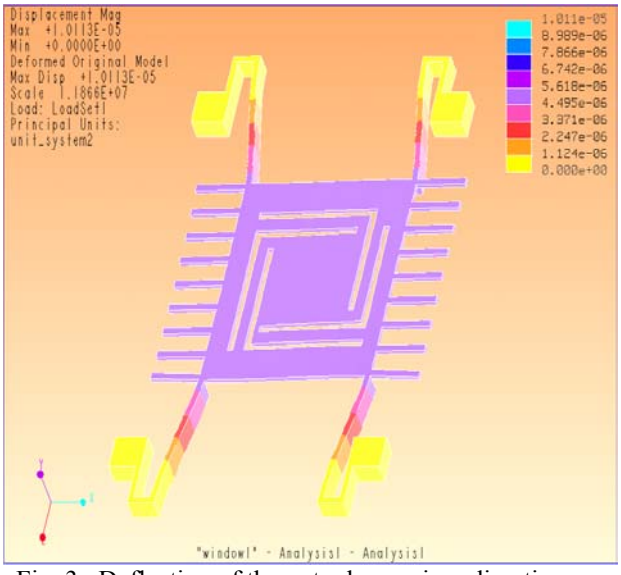

Fig. 3. Deflection of the outer beams in *x*-direction.

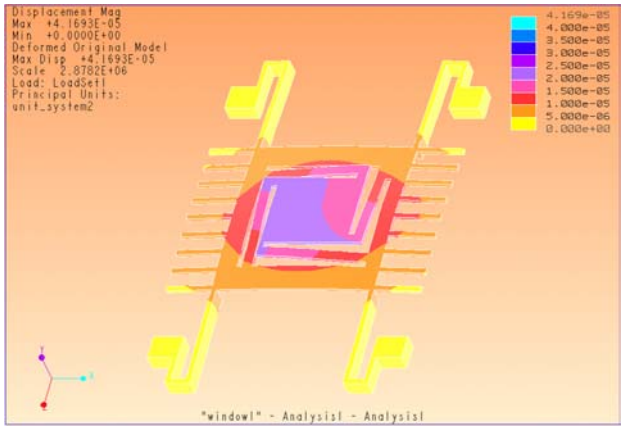

Fig. 4. Deflection of the inner beams in *y*-direction

3. DYNAMIC MODEL FOR CONTROLLER DESIGN

Referring to the lumped model of the vibrating gyroscope in Figure 5, and assuming that the angular rate Ω is constant, the equations of motion for the gyroscope can be written as:

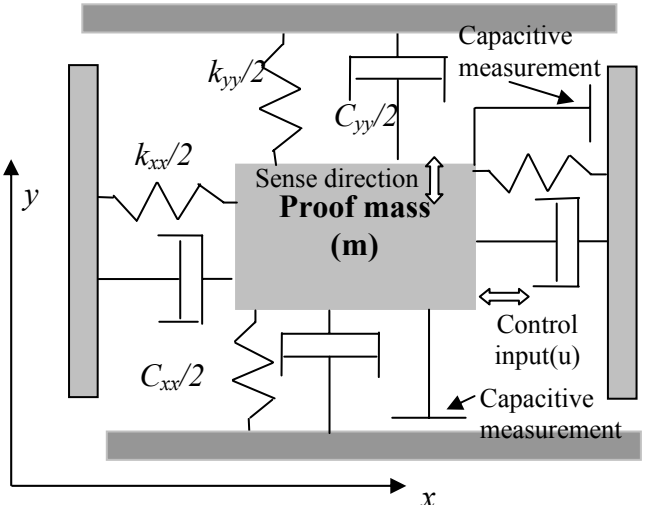

Fig. 5. The lumped model of the vibrating gyroscope

$$m\ddot{x} + C_{xx}\dot{x} + k_{xx}x + C_{xy}\dot{y} + k_{xy}y = u + 2m\Omega\dot{y} \quad (1)$$

$$m\ddot{y} + C_{yy}\dot{y} + k_{yy}y + C_{xy}\dot{x} + k_{xy}x = -2m\Omega\dot{x} \quad (2)$$

Where m is the vibrating mass, x and y are the coordinates of the proof mass relative to the fixed frame, k_{xx}, k_{yy}, k_{xy}, are the spring coefficients for the x and y coordinates and the coupling respectively. Similarly, the parameters C_{xx}, C_{yy}, C_{xy}, are the damping coefficient for the x and y coordinates and the cross coupling, respectively; $u(t)$ is the electrostatic driving force, Ω is the unknown angular

velocity to be measured, and $2m\Omega y^{\bullet}, -2m\Omega x^{\bullet}$ are the coupling forces due to the Coriolis effect.

The parameters of the lumped model (1)-(2) are estimated by simulating the vibrating gyroscope in Pro-E and Pro-Mechanica. Application of step input type forces to the proof mass in *x* and y-directions generate responses from the gyroscope through which the unknown coefficients $[k_{xx}, k_{yy}, k_{xy}, C_{xx}, C_{yy}\ C_{xy}]$ can be estimated under the assumption that the response of the distributed system in Figure 2 can be approximated by the lumped model of Figure 5. Only the structural damping is assumed to exist in the distributed model. The damping effect due to squeeze film and Couette flows are assumed negligible. This last assumption can be justified if the proof-mass is vibrating under vacuum. Following the usual convention, (1) and (2) are further transformed into forms where the quality factors (q, q_1, q_2) corresponding to the damping coefficients characterize the dynamics as in (3) – (4) below:

$$x^{\bullet\bullet} + \frac{\omega_n}{q} x^{\bullet} + \omega_n^2 x + \frac{\omega_{n2}}{q_2} y^{\bullet} + \omega_{n2}^2 y = u + 2\Omega y^{\bullet} \tag{3}$$

$$y^{\bullet\bullet} + \frac{\omega_{n1}}{q_1} y^{\bullet} + \omega_{n1}^2 y + \frac{\omega_{n2}}{q_2} x^{\bullet} + \omega_{n2}^2 x = -2\Omega x^{\bullet} \tag{4}$$

Where:

$\frac{\omega_n}{q} = \frac{C_{xx}}{m}$, $\omega_n = \sqrt{\frac{k_{xx}}{m}}$ is the natural frequency in the x-direction,

$\frac{\omega_{n2}}{q_2} = \frac{C_{yy}}{m}$, $\omega_{n1} = \sqrt{\frac{k_{yy}}{m}}$ is the natural frequency in the y-direction, (sense direction.)

$\frac{\omega_{n1}}{q_1} = \frac{C_{xy}}{m}$, $\omega_{n2} = \sqrt{\frac{k_{xy}}{m}}$ is the frequency due to coupling and (q, q_1, q_2) are the quality factors in x and y and coupling directions, respectively. Ω is the quantity of interest on this angular velocity measurement device and this quantity complicates the controller design since it appears as an unknown term in (3)-(4).

3. CONTROLLER DESIGN FOR THE VIBRATING GYROSCOPE

The control problem in a vibrating gyroscope is to maintain the proof mass to oscillate in *x*-direction at a given frequency and amplitude despite the facts that the motions in *x* and *y* directions are coupled and the angular frequency Ω is unknown. Typically the desired motion trajectory in *x*-direction is specified as

$$x_d = A\sin\omega_n t \tag{5}$$

Alternatively the desired motion can also be expressed as

$$x_d^{\bullet\bullet} = -A\omega_n^2 \sin\omega_n t = -\omega_n^2 x_d \tag{6}$$

By comparing (6) and (3) it is easy to see that the control signal given below

$$u = \frac{\omega_n}{q} x^{\bullet} + \omega_n^2 x + \frac{\omega_{n2}}{q_2} y^{\bullet} + \omega_{n2}^2 y - 2\Omega y^{\bullet} + \nu \tag{7}$$

with

$$\nu = -Be^{\bullet} - \omega_n^2 x \tag{8}$$

generates the desired motion specified in (6). In (8,) the parameter *B* is chosen to introduce controllable damping into the error dynamics which will be shown explicitly in (12) , later.

Obviously the solution (7) assumes that the states $(x, \dot{x}, y, \dot{y})$ and Ω are available to the controller. However, since the angular velocity Ω is unknown and it is indeed the quantity that needs to be determined, one has to consider the adaptive control design techniques [4-6] in order to solve the control problem.

In terms of an estimated angular velocity $\hat{\Omega}$, the controller (7) becomes:

$$u = \frac{\omega_n}{q} x^{\bullet} + \omega_n^2 x + \frac{\omega_{n2}}{q_2} y^{\bullet} + \omega_{n2}^2 y - 2\hat{\Omega} y^{\bullet} + \nu \tag{9}$$

re-arranging equations (6)-(8) gives:

$$x^{\bullet\bullet} - x_d^{\bullet\bullet} = \omega_n^2 x_d + 2\left(\Omega - \hat{\Omega}\right) y^{\bullet} + \nu \tag{10}$$

and by defining the tracking error $e = x - x_d$, (10) can be written as

$$e^{\bullet\bullet} + \omega_n^2 e = \omega_n^2 x + 2\left(\Omega - \hat{\Omega}\right) y^{\bullet} + \nu \tag{11}$$

Substituting ν from (8), the tracking error dynamics takes the form

$$e^{\bullet\bullet} + Be^{\bullet} + \omega_n^2 e = 2\left(\Omega - \hat{\Omega}\right)y^{\bullet} \tag{12}$$

Since both $B>0$ and $\omega_n>0$ the error will approach to zero if Ω is known exactly. In order to analyze the stability of the error equation (12) the following Lyapunov function is defined

$$V = \gamma_1 e^2 + \gamma_2 e^{\bullet^2} + \left(\Omega - \hat{\Omega}\right)^2 \quad \gamma_1, \gamma_2 > 0 \tag{13}$$

Further, introducing the measurement error $\delta = \left(\Omega - \hat{\Omega}\right)$, the derivative of the Lyapunov function becomes

$$\dot{V} = (2\gamma_1 - 2\gamma_2\omega_n^2)e\dot{e} - 2\gamma_2 B\dot{e}^2 + (\Omega - \hat{\Omega})(4\gamma_2 \dot{e}y - 2\dot{\hat{\Omega}}) + (\Omega - \hat{\Omega})^2 \dot{y}y \tag{14}$$

In order to maintain a bound on the control error e and the estimation error δ one requires $\dot{V} \le 0$ which can be achieved by choosing

$$2\gamma_1 - 2\omega_n^2\gamma_2 = 0 \tag{15}$$

$$\gamma_2 = 1\,, \quad \gamma_1 = \omega_n^2, \text{ and} \tag{16}$$

$$4\gamma_2 y^{\bullet} e^{\bullet} + 2\delta^{\bullet} = 0 \tag{17}$$

If $\hat{\Omega}$ is small and within close vicinity of Ω, i.e., . $(\Omega - \hat{\Omega})^2 \cong 0$ then $V^{\bullet} = -2Be^{\bullet^2} \le 0$.

An estimate of the angular velocity, $\hat{\Omega}$ can be obtained from (17) and the definition $\delta = \left(\Omega - \hat{\Omega}\right)$ which result in the following expression to estimate the angular velocity Ω.

$$\frac{d\hat{\Omega}}{dt} = -2y^{\bullet}\left(x^{\bullet} - x_d^{\bullet}\right) \tag{18}$$

Figures 6a, 6b show the behavior of the Lyapunov function. The results are obtained by simulating the lumped model (3)-(4) under the controller (9) operating with the estimation algorithm (18). The parameters of the lumped model are given in the Appendix. It is easy to see that that the Lyapunov function is decreasing but not necessarily reaching zero exactly since the integration in (18) is performed numerically. The negative semi-definite Lyapunov function guarantees that all signals in the controlled system will be bounded and therefore the estimation error $\delta = \left(\Omega - \hat{\Omega}\right)$ will also be remained bounded but it is difficult to establish conditions for convergence to zero. In fact, Figure 7 shows that the estimation error remains bounded but does not necessarily converge to zero.

An alternative approach to obtain a better estimate of the angular velocity Ω can be formulated as follows. Since the Lyapunov based controller (9) makes sure that the tracking error $e = x - x_d$ goes to zero, as evident from Figure 8, then upon substitution of

$x = x_d = A\sin\omega_n t$ into (4), the proof mass dynamics in y-direction takes the form,

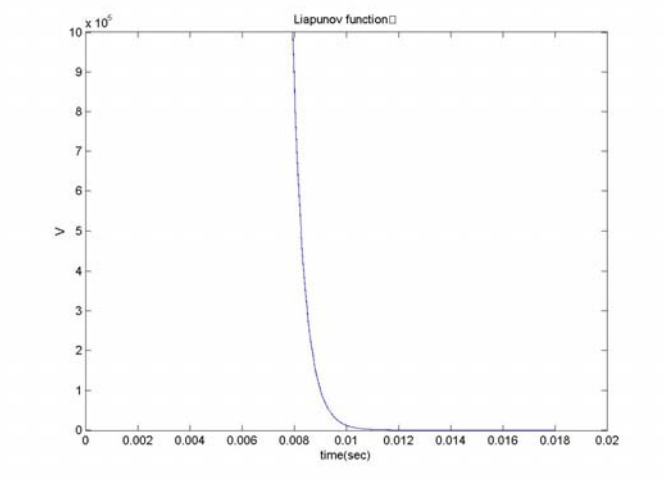

Fig. 6a. Convergence of the Lyapunov function

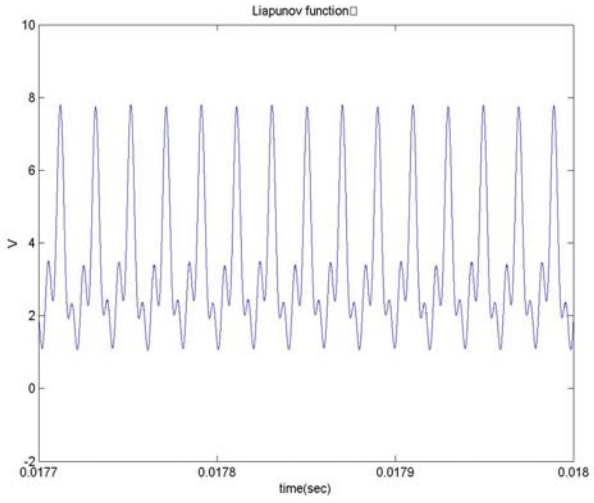

Fig. 6b. The Lyapunov function expanded in the final convergence region.

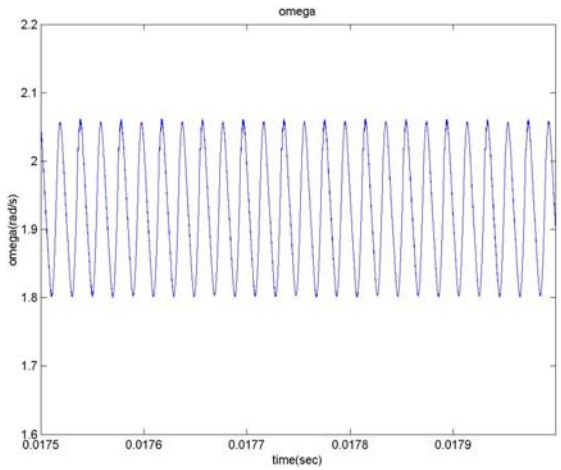

Fig. 7: Estimated angular speed $\hat{\Omega}$, the true value is $\Omega = 1\ rad/\sec$

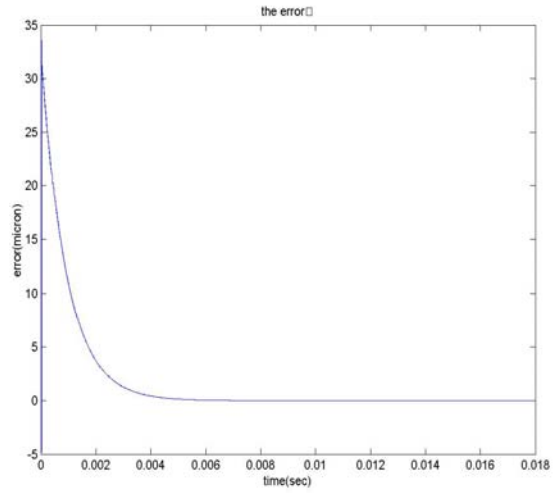

Fig. 8. Convergence of the tracking error *e(t)* to zero.

$$y'' + \frac{\omega_{n1}}{q_y} y' + \omega_{n1}^2 y = -\omega_{n2} A\omega_n \cos\omega_n t - \omega_{n2}^2 A \sin\omega_n t - 2\Omega A\omega_n \cos\omega_n t \tag{19}$$

which can be simplified to:

$$y'' + \frac{\omega_{n1}}{q_y} y' + \omega_{n1}^2 y = C_1 \sin\ \omega_n t + C_2 \cos\ \omega_n t \tag{20}$$

where:

$$C_1 = -\frac{k_{xy}}{m} A, \text{ and}$$

$$C_2 = -\frac{C_{xy}}{m} A\omega_n - \frac{2\omega_n}{m} A\Omega \tag{21}$$

The Laplace transform of (20) gives the steady state solution :

$$y(t) = C_1 \frac{1}{|D(j\omega_n)|} \sin(\omega_n t + \phi) + C_2 \frac{1}{|D(j\omega_n)|} \cos(\omega_n t + \phi) \tag{22}$$

where $D(s) = s^2 + \frac{\omega_{n1}}{q_y} s + \omega_{n1}^2$.

The measured output amplitude *y(t)* reaches its maximum at:

$$\left(\frac{y_{max}}{A}\right)^2 = C_1^2 + C_2^2 \tag{23}$$

with $A = \frac{1}{|D(j\omega_n)|}$.

Since y_{max} is a measurable quantity then the unknown angular velocity Ω can be determined from (23) and (21) by solving for Ω.

Figure 9 shows the simulated response of the MEMS gyroscope in the y-direction for an input angular velocity of $\Omega = 1\ rad/\sec$. The parameters of the system are again the same as listed in the Appendix. The estimated angular velocity is found to be $\hat{\Omega} = 0.997\ rad/\sec$. which corresponds to an estimation error of 0.24%.

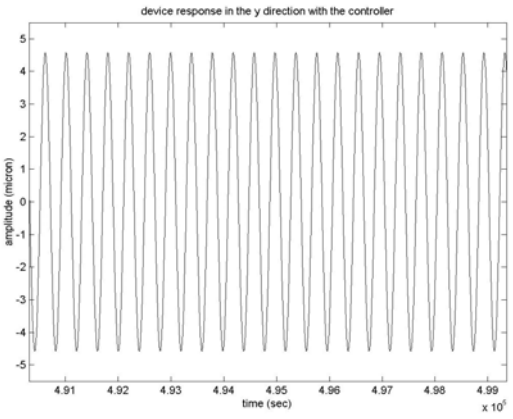

Fig. 9: y-direction motion of the proof mass

5. CONCLUSIONS

There is an inevitable cross-coupling between the orthogonal axes of a vibrating MEMS gyroscope. Furthermore the quantity that one wants to measure, i.e. the angular velocity of the proof mass, becomes an unknown disturbance term to the controller, which tries to maintain the proof mass to vibrate at fixed amplitude and frequency. In order to solve this problem an adaptive control system formulation has been used which simultaneously estimates the unknown angular velocity and controls the motion of the proof mass.

It has been shown both analytically and through numerical simulations that a Lyapunov function based controller can maintain the proof mass at the desired amplitude and frequency therefore the tracking error goes to zero. Furthermore all signals within the control system, including the estimation error, remain bounded. However, despite the fact that the tracking error goes to zero, there is no guarantee that the estimation of the angular velocity will approach to the true value since the Lyapunov stability theorem can only guarantee the boundedness of signals.

In order to obtain consistent estimates of the unknown angular velocity a new technique has been proposed which takes advantage of the fact that the tracking error goes to zero. The proposed technique has been demonstrated through simulations on a modified MEMS gyroscope proposed by Yoichi et al [2].

If the uncertainties of the system can be estimated, then sliding mode controller on the drive direction and a force balance controller on the sense direction can be constructed to consistently estimate the unknown angular velocity. This work is currently being developed and will be reported in the conference.

REFERENCES

1. Khasawneh Q. (2002), Adaptive control for a simulated micro electro mechanical vibrating gyroscope, University of Akron, Akron, OH
2. Yoichi M., Masaya T, Kuniki O. (2000), "A micromachined vibrating rate gyroscope with independent beams for the drive and detection modes", Sensors and Actuators, 80, pp 170-178.
3. Ljung P.B. (1997), "Micromachined Gyroscope with Integrated Electronics", PhD Thesis, The University of California, Berkeley.
4. Sastry S., Bodson M. (1989), " Adaptive Control, Stability, Convergence, and Robustness", Prentice Hall.
5. Watanabe K. (1992), " Adaptive Estimation and Control", Prentice Hall.
6. Kumpati S., Anuradha M. (1989), " Stable Adaptive Systems", Prentice Hall.

APPENDIX

Model parameters which are used in the simulations are as follows.

$$\omega_n = 1.58e5Hz$$
$$\omega_{n1} = 5.94e4Hz$$
$$\omega_{n2} = 1.82e4Hz$$
$$q_x = 100$$
$$q_y = 100$$
$$q = 100$$
$$\text{Mass} = 7.55012e-6(g)$$
$$A = 50 micron$$
$$y_{max} = 76.3 \ micron$$
$$\Omega = 1 \ rad/\sec$$
$$K_{xx} = 1.90e-5g/s^2$$
$$K_{yy} = 2.67e-4g/s^2$$
$$K_{xy} = 2.5e-3g/s^2$$